Arch. Min. Sci. **66** (2021), 2, 265-278

Electronic version (in color) of this paper is available: http://mining.archives.pl

DOI 10.24425/ams.2021.137461

ZHU BAIRU[1], SONG YANG[1],
WU BEINING[1], LI YONGQI[1*]

EXPERIMENTAL STUDY ON THE EFFECTS OF VIBRATIONAL FREQUENCY ON THE PERMEABILITY OF GAS-CONTAINING COAL ROCKS

Low-frequency mechanical vibrations can trigger disasters such as coal-gas outbursts. An in-house "vibration-triaxial stress-seepage" experimental apparatus was used to measure the gas flow rate of rock specimens with varying vibrational frequency, gas pressure, and confining pressure. The results of these tests were then used to derive expressions that describe how the permeability of gas-containing coal rocks is related to these aforementioned factors. In addition, sensitivity coefficients were defined to characterise the magnitude of the permeability response to each permeability-affecting factor (i.e., vibrational frequency and gas pressure). The following insights were gained, regarding the effects of vibrational frequency on the permeability of gas-containing coal rocks: (1) If gas pressure and confining pressure are fixed, the permeability of gas-containing coal rocks rapidly increases, before gradually decreasing, with increasing vibrational frequency. Thus, the permeability of the gas-containing coal rock is always larger with vibrations than without. (2) If vibrational pressure and confining pressure are fixed, the relationship between the permeability of gas-containing coal rocks and gas pressure is consistent with the "Klinkenberg effect," i.e., the permeability initially decreases, and then increases, with increasing gas pressure. (3) The change in permeability induced by each unit change in gas pressure is proportional to the gas pressure sensitivity coefficient. (4) The change in permeability induced by each unit change in vibrational frequency is proportional to the vibrational frequency sensitivity coefficient.

Keywords: gas-containing coal rock, low-frequency vibration, gas pressure, permeability, sensitivity coefficient

1. Introduction

Permeability indicates how difficult it is for gas to seep through a coal seam; this indicator is necessary to prevent and mitigate coal-gas outbursts [1,2]. Hence, in-depth studies on coal-

[1] LIAONING TECHNICAL UNIVERSITY, SCHOOL OF CIVIL ENGINEERING, FUXIN, LIAONING, 123000, CHINA

* Corresponding author: 2075206667@qq.com

gas seepage in coal seams have a theoretical and practical significance in the discernment of the triggering mechanisms of coal-gas outbursts and the prediction of these disasters. The seepage of coal-gas has been investigated via theoretical and experimental approaches by researchers around the world. The following four mainstream seepage theories have been established after many years of theoretical study: linear seepage theory, non-linear seepage theory, the theory of seepage in geophysical fields, and multi-seam gas seepage theory [3-5]. In experimental studies, researchers have investigated the effects of ground stress, temperature, gas pressure, adsorption/desorption, mining-induced stresses, and coal quality on the permeability of gas-containing coal rocks [6-8] discovered that the rate of gas seepage and its response to temperature changes are related to the changes in internal energy and structure of loaded coal bodies. Hence, the rate of gas seepage, and its response to temperature, can be used as warnings for the destabilisation or failure of coal bodies. [9] used an in-house experimental system to investigate the effects of water content on gas seepage. It was found that gas seepage is related to water content by a negative exponential. [10] compared coal briquettes and raw coal in terms of the effects of temperature on their respective permeabilities; they found that coal permeability generally decreases with increasing temperature. It is known that the effects of these factors on gas seepage are not simple or monotonous [11-13] have studied the permeability trends of gas-containing coal rocks in the presence of heat-flow-solid coupling. [6], [14] and [15] have corrected seepage models and performed experiments and simulations to study the extent to which coal-gas seepage is affected by known influencing factors.

Recent studies show that coal-gas outbursts can not only be induced by the low-frequency mechanical vibrations that are produced by excavation works, air picks, and hole boring, but also by gas pressure and ground & mining-induced stress. This is because low-frequency mechanical vibrations affect the flow of the coal-gas in a coal seam [16,17]. Very few studies regarding the effects of low-frequency mechanical vibrations on the permeability of gas-containing coal rocks have been performed. However, the only study concerning these effects is that by [16] and [18], which focused on the effects of low-frequency mechanical vibrations on the adsorption-desorption processes of gas-containing coal rocks in the absence of external stress. However, this study does not account for the effects of low-frequency mechanical vibrations on the permeability of gas-containing coal rocks in the presence of triaxial stress.

Therefore, we have conducted a detailed investigation into the effects of low-frequency mechanical vibrations on the permeability of gas-containing coal rocks under triaxial stress by using an in-house “vibration-triaxial stress-seepage” experimental apparatus. Sensitivity coefficients were also defined for gas pressure and vibrational frequency in order to describe the magnitude of the permeability response to changes to these factors. This study was purposed to reveal the permeability characteristics of gas-containing coal rocks under the influence of low-frequency vibrations.

2. Experimental apparatus

The effects of low-frequency mechanical vibrations on the permeability of gas-containing coal rocks were investigated by using an in-house experimental apparatus. The test system consists of four parts, the test generating system for loading the specimen, the excitation system for applying controllable external vibration force to the specimen, the pressure loading system and the monitoring system. The test system mainly includes core holder, modal exciter, signal gen-

erator with built-in power amplifier, gas loading device, confining pressure loading device, axial pressure loading device, flow monitoring device, etc. [19,20]. A schematic of the experimental apparatus is shown in Fig. 1. In this figure, 1 is a core holder, 2 is a modal exciter, 3 is the signal generator of a built-in power amplifier, 4 is a high-pressure gas cylinder, 5 is a pressure gauge, 6 is a six-way valve, 7 is a force pump, and 8 is a flow monitor.

The primary parameters of the experimental apparatus are as follows:

(1) Confining pressure: 0-32 MPa, accuracy: ±0.1 MPa.
(2) Axial pressure: 0-32 MPa, accuracy: ±0.1 MPa.
(3) Range of output frequencies: 2-20 kHz, accuracy: ±0.1 Hz.
(4) Dimensions of the experimental chamber: Φ25 × 25 mm ~Φ25 × 80 mm.

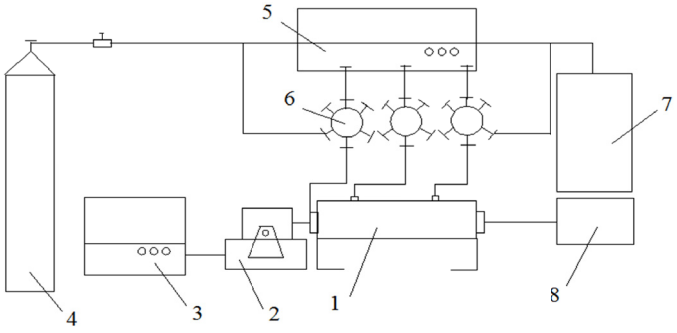

Fig. 1. Schematic of the experimental apparatus

The specific technical parameters of core gripper, vibration exciter, signal generator with built-in power amplifier and other experimental equipment used in this test are shown in Table 1.

TABLE 1

Relevant technical parameters of test equipment

Test equipment	Name of technical index	Technical parameter value
Core holder	Overall stiffness of the machine	7×109 N/m
	Working pressure	32 MPa
	Working temperature	180℃
Vibration exciter	Maximum exciting force	20 N
	Maximum amplitude	3 mm
	Maximum frequency	15 kHz
	Output mode	Ejector
	Maximum acceleration	20 g
Signal generator	Output frequency range	2-20 kHz
	Output waveform	Sine wave, square wave, triangle wave, white noise
	power output	30 w
	Display frequency	0-99999 Hz

3. Experimental methods and procedures

3.1. Specimen preparation

The coal specimens used in this experiment were sourced from the Shanxi Datong Coal Mine. First, a Φ25-mm core barrel and core-drilling machine were used to obtain approximately 50-mm-long cores. A core polishing machine was then used to shape and polish these cores into Φ25 × 50 mm raw coal samples. After the residual coal dust was wiped off of the sample surfaces, the samples were wrapped in cling wrap and stored in a dry and ventilated environment. Some of the samples are shown in Fig. 2.

Fig. 2. Photograph of some of the samples

3.2. Experimental procedure

The experimental apparatus shown in Fig. 1 was used to investigate gas seepage in coal samples at varying vibrational frequency (0, 10, 20, 30, 40, and 50 Hz), gas pressure (0.2, 0.3, 0.4, 0.5, 0.6, 0.7, 0.8, 0.9, 1.0, 1.1, 1.2, 1.3, 1.4, 1.5, 1.6, 1.7, 1.8, 1.9, and 2.0 MPa), and confining/axial pressure (4 MPa, 6 MPa and 10MPa). The energy of the vibration in the test is proportional to the square of its amplitude. There are 18 cases in the test, as shown in Table 2. Each case needs to be tested three times, and a total of 54 test samples are required. 99.99% nitrogen gas was used as the gaseous medium, and the experiments were performed at a constant temperature of 37°C. The experimental procedure was as follows:

(1) All intake valves, in addition to the valve connected to the pressure gauge, were opened, while the remaining valves were kept closed. The experimental chamber was then filled with nitrogen gas up to a pressure of 3 MPa. Under these conditions, a change in measured pressure implies that the experimental apparatus is leaky. When this occurred, actions were taken to repair the leak, and the air-tightness of the experimental system was then inspected; this process was repeated until the measured pressure was stable.

(2) After the sample was installed in the chamber inside the core holder, a wrench was used to tightly close the lid of the chamber. The chamber was then connected to a high-pressure pipeline, which was connected to a flow monitor.
(3) All of the valves that control axial pressure and confining pressure were opened, and a force pump was used to slowly increase the axial pressure and confining pressure of the sample up to 4 MPa; this was purposed to simulate a hydrostatic pressure environment. The control valves were shut after the axial and confining pressures stabilised.
(4) The pressure loading valve was then opened, and the gas pressure was increased to one of the 19 aforementioned gas pressure values. The measurement of gas flow was initiated after the gas bubbles discharged by the outlet tube became uniform and stable; the gas flow was measured three times at each level of gas pressure.
(5) One of the core-holder chamber covers was removed to change the sample. The high-pressure pipeline was then reconnected, and the modal exciter and signal generator were activated. Vibrations were applied to the sample for 500 s at one of the five aforementioned vibrational frequencies. Step (4) was then repeated at the end of each vibration experiment.
(6) After all 4-MPa confining/axial pressure experiments were completed, Steps (4) and (5) were repeated with confining/axial pressures of 6 and 10 MPa. The experiment concluded after measurements were obtained under all of the aforementioned pressure conditions.

TABLE 2

Test plan

Test piece No	**Confining pressure and axial pressure /MPa**	**Vibration frequency /Hz**	**Gas pressure (interval 0.1MPa)/MPa**
A-1	4	0	0.2-2.0
A-2		10	
A-3		20	
A-4		30	
A-5		40	
A-6		50	
B-1	6	0	
B-2		10	
B-3		20	
B-4		30	
B-5		40	
B-6		50	
C-1	10	0	
C-2		10	
C-3		20	
C-4		30	
C-5		40	
C-6		50	

3.3. Method to calculate permeability

The time taken for the gas to drain water from a coal sample (drainage time) was measured under various experimental conditions; the drainage times corresponding to each experimental condition were averaged after all invalid measurements were excluded. The gas flow corresponding to each experimental condition was calculated by applying the drainage time and range of measurement of the measuring cylinder. The permeability of the sample was then calculated by using the permeability equation. Please note that the steady-state gas flow was calculated by using the volume of the measuring cylinder, V, and the drainage time, t, i.e., $Q_1 = V/t$.

In this experiment, it was assumed that the migration of gas in the coal sample was an isothermal process that satisfies the ideal gas law. Based on Boyle's law and Darcy's law, the permeability of a coal sample is expressed as [21,22].

$$K = \frac{2\mu p_0 Q_1 L}{A\ p_1^2 - p_2^2} \tag{1}$$

In this equation, K is the permeability of the coal sample in 10^{-10} m^2; μ is the absolute viscosity of the gas, which is 1.35×10^{-5} pa · s; p_0 is the atmospheric pressure of the laboratory, which is 0.1 MPa; Q_1 is the steady-state gas flow in cm^3/s. L is the length of the specimen, which is 50 mm; A is the cross-sectional area of the sample, which is 4.91 cm^2; p_1 is the inlet pressure of the sample in MPa; p_2 is the outlet pressure of the sample, which is 0.1 MPa.

4. Analysis of experimental results

4.1. Mechanisms by which gas pressure affects the permeability of gas-containing coal rocks

At vibrational frequencies of 0, 10, 20, 30, 40, and 50 Hz, the permeability of a coal rock sample varies according to gas pressure, as shown in Fig. 3. An expression for the relationship between permeability and gas pressure was obtained by fitting the experimental data, as shown below:

$$k = y_0 + \frac{z}{w \cdot \sqrt{\pi / 2}} \cdot e^{\left[-2\left(\frac{p-xc}{w}\right)^2\right]} \tag{2}$$

In this equation, y_0, xc, w, and z are fitting parameters.

Based on the permeability-versus-gas pressure plots shown in Fig. 3 and Eq. (2), it may be that, under the conditions that the vibrational frequency and confining pressure are fixed, the permeability initially decreases, and then increases, with increasing gas pressure. This "V"-shaped plot is consistent with the Klinkenberg effect; these results also show that the critical gas pressure of the Klinkenberg effect is approximately 0.9 MPa in this experiment. When the gas pressure is constant, the permeability decreases with the increase of confining pressure.

This phenomenon is caused by imbalances between the deformations associated with gas adsorption-induced coal swelling, which narrows the pores/cracks of the coal body, and

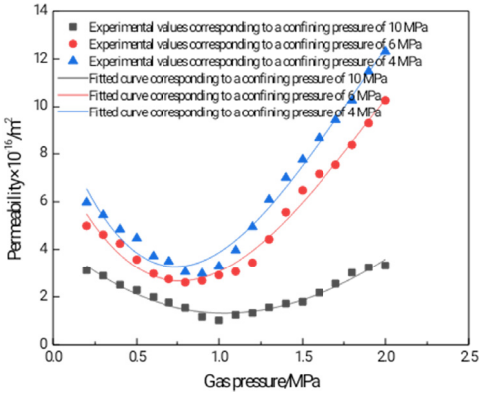

(a) Vibrational frequency of 0 Hz

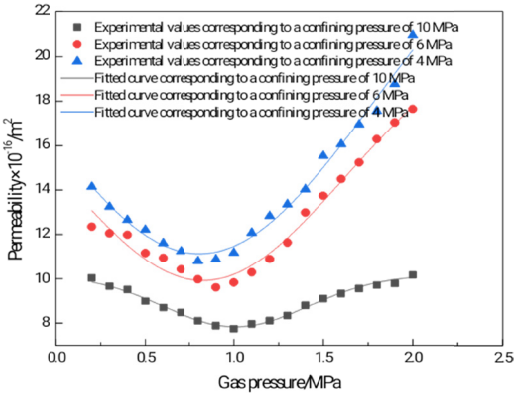

(b) Vibrational frequency of 10 Hz

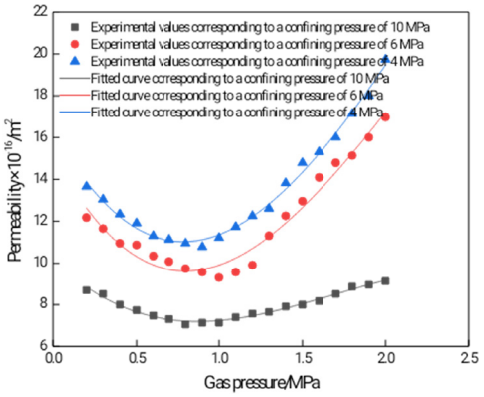

(c) Vibrational frequency of 20 Hz

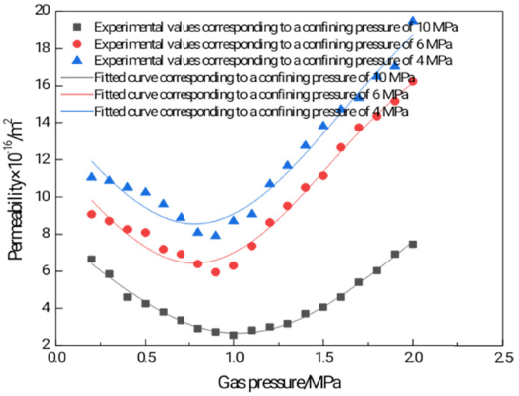

(d) Vibrational frequency of 30 Hz

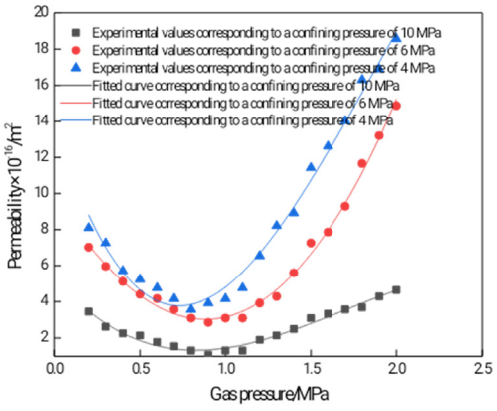

(e) Vibrational frequency of 40 Hz

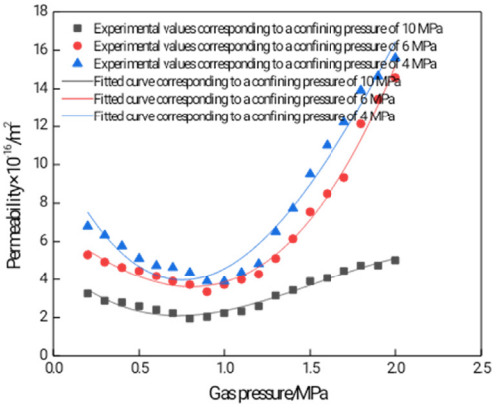

(f) Vibrational frequency of 50 Hz

Fig. 3. Experimental and fitted permeability-versus-gas pressure plots
with varying vibrational frequency and confining pressure

gas pressure-induced coal skeleton compression, which expands the internal pores and cracks of the coal body. At low gas pressures, an increase in gas pressure leads to larger amounts of adsorption-induced coal swelling than pressure-induced coal skeleton compression; because the deformations of the former are greater than those of the latter, the Klinkenberg effect is significant at low gas pressures. After gas pressure exceeds the critical point, further increases in gas pressure lead to greater amounts of pressure-induced coal skeleton compression than adsorption-induced coal swelling; because the deformations of the latter are greater than those of the former, the Klinkenberg effect gradually disappears at high gas pressures. According to Reference [23]. [24] the critical point of the Klinkenberg effect is dependent on the type of coal, coal quality, pore pressure and stress state of the coal rock. According to the seepage measurements in this experiment, the critical point is altered by changes in confining pressure. Nonetheless, the critical point generally occurs at approximately 0.9 MPa.

4.2. Mechanism by which vibrational frequency affects the permeability of gas-containing coal rocks

At gas pressures of 0.5, 1.0, 1.5, and 2.0 MPa, the permeability was observed to vary with vibrational frequency, as illustrated in Fig. 4. An expression for the relationship between permeability and vibrational frequency was obtained by fitting the experimental data, as shown below:

$$K = c\omega^3 + d\omega^2 + e\omega + f \tag{3}$$

In this equation, c, d, e, and f are fitting parameters.

As shown in Fig. 4, under the condition that gas pressure and confining pressure are fixed, the permeability of gas-containing coal rocks first increases, then decreases with increasing vibrational frequency. At vibrational frequencies below 10 Hz, the permeability rapidly increases with increasing vibrational frequency until a peak is reached. Further increases in vibrational frequency lead to a gradual decrease in permeability until a constant value is reached. This describes the overall trend by which permeability varies with vibrational frequency. Hence, permeability initially increases and then decreases with increasing vibrational frequency. In all cases, under the condition of vibration, the permeability of coal is higher than that of coal without vibration (i.e. the vibrational frequency is 0 Hz). Therefore, vibrations increase the permeability of gas-containing coal rocks.

At the initial stage of vibration, the raw coal is affected by vibration, which leads to the expansion of existing cracks and the increase of porosity in the raw coal, thus increasing the permeability of coal and rock. The porosity and permeability of the coal rocks will therefore rapidly increase, with increasing vibrational frequency during this stage. This leads to permeability being maximised after a small increase in vibrational frequency. If the vibrational frequency is further increased, the compressive forces generated by the vibrations will compress the pores of the coal body and ultimately reduce its porosity and permeability; this effect becomes stronger as the vibrational frequency is increased. As the vibrational frequencies applied in this experiment are relatively low, the vibrations did not produce plastic deformations or large cracks in the coal samples. Furthermore, the cracks inside the coal samples did not extend to the exterior. Hence, the vibrations that were applied during this experiment only produced compressive actions

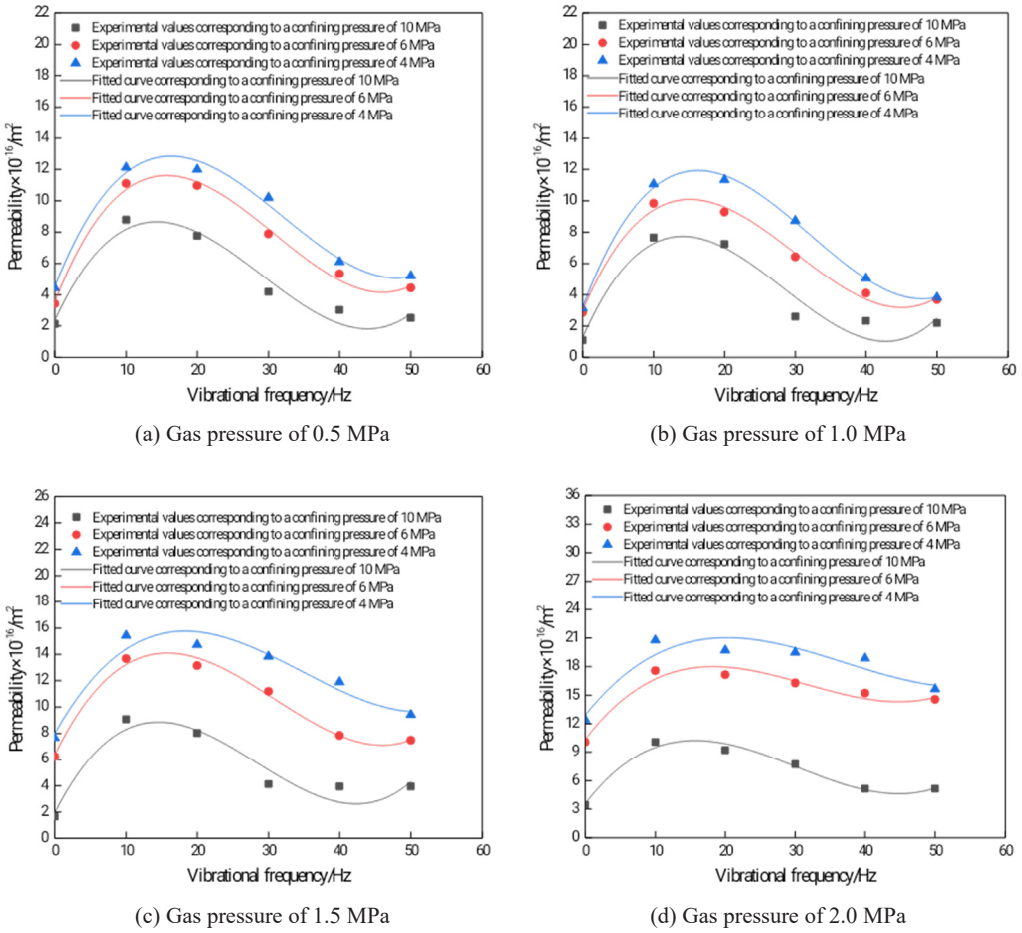

(a) Gas pressure of 0.5 MPa

(b) Gas pressure of 1.0 MPa

(c) Gas pressure of 1.5 MPa

(d) Gas pressure of 2.0 MPa

Fig. 4. Experimental and fitted permeability-versus-vibrational frequency plots with varying gas pressure and confining pressure

within the coal body, and the permeability of the coal samples trended towards a fixed value as the vibrational frequency was increased.

4.3. Sensitivity of coal permeability to gas pressure

In this work, the gas pressure sensitivity coefficient is defined as the absolute change in permeability resulting from a unit increase in gas pressure, under some constant confining pressure. In other words, our gas pressure sensitivity coefficient is a modification of the sensitivity coefficient defined by Xu et al., with the modification being the inclusion of absolute permeability values. The modified sensitivity coefficient provides a clearer description of the degree by which gas pressure affects permeability. The equation used to calculate the gas pressure sensitivity coefficient is as follows:

$$C_p = \left| \frac{1}{K_0} \frac{\partial K}{\partial p} \right| \tag{4}$$

In this equation, C_p is the gas pressure sensitivity coefficient, K_0 is the initial permeability of the rock sample in m^2, ∂K is the change in permeability in m^2, and ∂p is the change in gas pressure in MPa.

According to Eqs. (2) and (4), the gas pressure sensitivity coefficient, C_p, is related to gas pressure, p, by the following equation:

$$C_p = \left| \frac{4z(p - xc)}{k_0 w^3 \sqrt{\pi / 2}} \cdot e^{\left[-2\left(\frac{p - xc}{w} \right)^2 \right]} \right| \tag{5}$$

In this equation, y_0, xc, w, and z are fitting parameters.

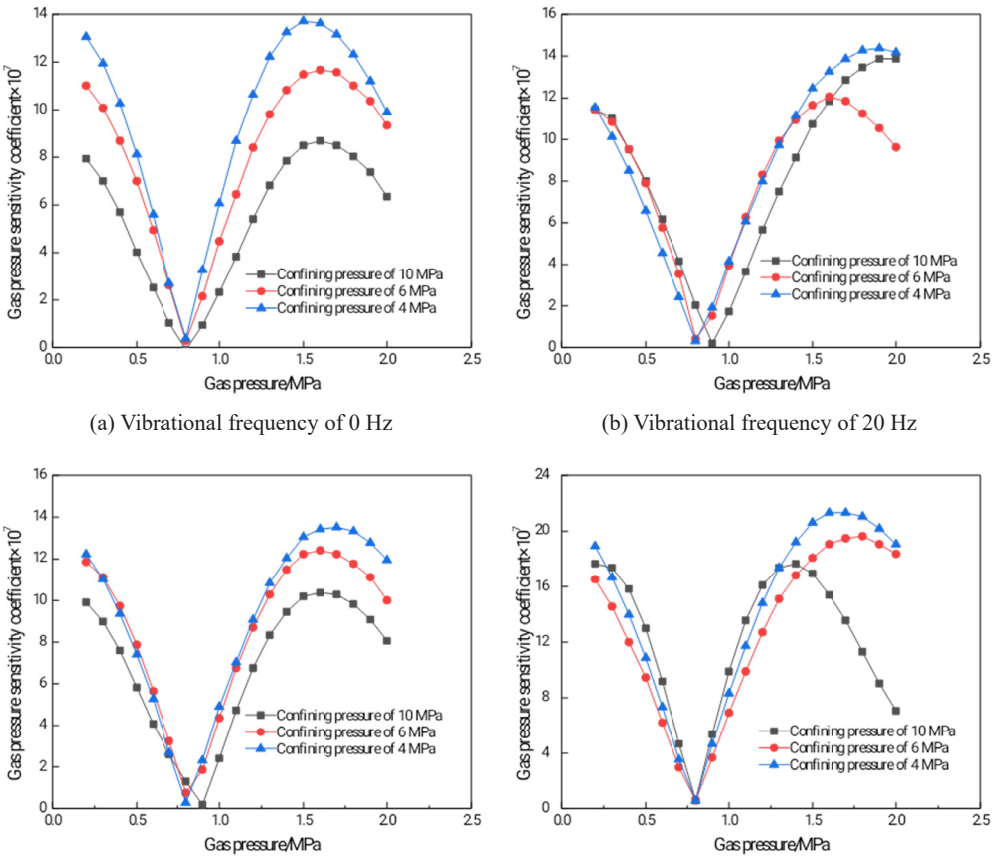

(a) Vibrational frequency of 0 Hz

(b) Vibrational frequency of 20 Hz

(c) Vibrational frequency of 40 Hz

(d) Vibrational frequency of 50 Hz

Fig. 5. Relationship between the gas pressure sensitivity coefficient and gas pressure for different vibrational frequencies

Eq. (5) can be used to calculate the C_p of a coal sample at each vibrational frequency and confining pressure. C_p was thus plotted against gas pressure, as shown in Fig. 5. It can be seen from Fig. 5 that under the condition of constant vibration frequency and confining pressure, with the increase of gas pressure, the sensitivity coefficient of gas pressure first decreases to the lowest value and then increases gradually.

Based on the results illustrated in Figs. 3 and 5, it may be inferred that the extent to which gas pressure affects permeability is proportional to C_p; the change in permeability with changes in gas pressure is therefore proportional to C_p. Hence, C_p characterses the magnitude of the permeability response to gas pressure.

4.4. Sensitivity of permeability to vibrational frequency

The vibrational frequency sensitivity coefficient is defined as the absolute change in permeability caused by a unit increase in vibrational frequency at some constant confining pressure. The vibrational frequency sensitivity coefficient may be expressed as follows:

$$C_K = \left| \frac{1}{K_0} \frac{\partial K}{\partial \omega} \right| \tag{6}$$

In this equation, C_K is the vibrational frequency sensitivity coefficient, K_0 is the initial permeability of the rock sample in m^2, ∂K is the change in permeability in m^2, and $\partial \omega$ is the change in vibrational frequency, Hz.

According to Eqs. (3) and (6), C_K is related to vibrational frequency, ω, by the following equation:

$$C_K = \left| \frac{3c\omega^2 + 2d\omega + e}{K_0} \right| \tag{7}$$

Eq. (7) can be used to calculate C_K for each value of gas pressure and confining pressure. C_K was thus plotted against vibrational frequency, as shown in Fig. 6.

By comparing the results in Figs. 4 and 6, it may be inferred that C_K quantitatively describes the extent to which the vibrational frequency affects permeability, showing that the effects of vibrational frequency on permeability are proportional to C_K, as is the magnitude of the corresponding changes in permeability.

5. Conclusions

Based on the experimental data, the influence of gas pressure, vibration frequency and vibration time on permeability, the sensitivity coefficient of gas pressure and vibration frequency is defined to quantitatively analyse the response of permeability to gas pressure and vibration frequency. The main conclusions are as follows:

(1) Under the condition of constant vibration frequency and confining pressure, the permeability first decreases, then increases with the increase of gas pressure. The relation-

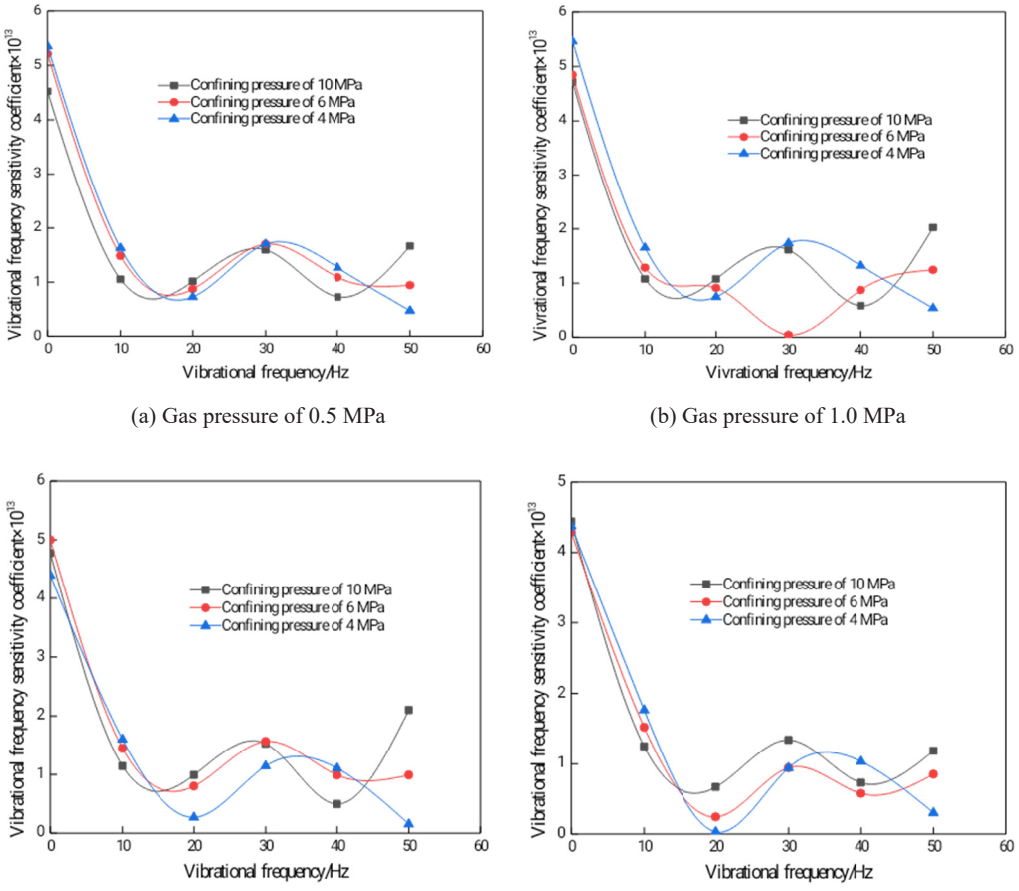

(a) Gas pressure of 0.5 MPa

(b) Gas pressure of 1.0 MPa

(c) Gas pressure of 1.5 MPa

(d) Gas pressure of 2.0 MPa

Fig. 6. Relationship between the vibrational frequency sensitivity coefficient and vibrational frequency for different gas pressures

ship between gas pressure and permeability in "V" shape conforms to the Klinkenberg effect, and the critical point of gas pressure is the Klinkenberg critical point, which is 0.9 MPa;

(2) Under the condition of constant gas pressure and confining pressure, the permeability of gas-bearing coal increases first and then decreases with the increase of vibration frequency; the influence of vibration frequency on permeability has a limit value, which reaches the maximum value when the vibration frequency is 10 Hz, and the permeability increases faster when the vibration frequency increases from 0 Hz to 10 Hz, and the vibration frequency increases from 10 Hz when the frequency increases to 50 Hz and the permeability decreases slowly;

(3) With the increase of vibration frequency, the permeability first increases rapidly and then decreases slowly. The increase of permeability is greater than the decrease of perme-

ability. The permeability with vibration frequency is greater than the initial permeability without vibration frequency, that is, the vibration frequency increases the permeability of coal;

(4) Under the condition of a certain vibration frequency, the permeability first decreases rapidly with the increase of vibration time, then decreases, and finally stabilises at a fixed value;

(5) By comparing and analysing the relationship curve between permeability and gas pressure and the relationship curve between gas pressure sensitivity coefficient and gas pressure, it can be seen that the larger the gas pressure sensitivity coefficient is, the larger the change range of permeability, the smaller the gas pressure sensitivity coefficient is, the smaller the change range of permeability and the smaller the gas pressure sensitivity coefficient is. The coefficient can quantitatively characterise the influence of gas pressure on permeability;

(6) By comparing and analysing the relationship between permeability, the vibration frequency and the relationship between vibration frequency sensitivity coefficient, it can be seen that the larger the vibration frequency sensitivity coefficient is, the larger the change in the range of permeability; the smaller the vibration frequency sensitivity coefficient is, the smaller the change range of permeability. The vibration frequency sensitivity coefficient can quantitatively characterise the influence of vibration frequency on permeability.

Acknowledgement

This paper was supported by the National Natural Science Foundation (51974146), Liaoning Natural Science Foundation (2019-ZD-0042).

References

[1] L. Zhou, L. Yuan, R. Thomas, A, Iannacchione, *Determination of Velocity Correction Factors for Real-Time Air Velocity Monitoring in Underground Mines*. Int. J. Coal Sci. Technol. **4** (4), 322-332 (2017). DOI: https://doi.org/10.1007/s40789-017-0184-z

[2] M. Ajamzadeh, V. Sarfarazi, H. Dehghani, *Evaluation of Plow System Performance in Long-Wall Mining Method Using Particle Flow Code*. Int. J. Coal Sci. Technol. **6** (4), 518-535 (2019). DOI: https://doi.org/10.1007/s40789-019-00266-3

[3] Y. Lei, Y. Zeng, Z. Ning, *Transient Flow Model of Multiply Fractured Horizontal Wells in Shale Gas Reservoirs and Well Test Analysis*. Fau-Blo Gas Field **25** (4), 477-483 (2018). DOI: https://doi.org/10.6056/dkyqt201804015

[4] D. Jamróz, T. Niedoba, A. Surowiak, *Application of Multi-Parameter Data Visualization by Means of Multidimensional Scaling to Evaluate Possibility of Coal Gasification*. Arch. Min. Sci. **62** (3), 445-457 (2017). DOI: https://doi.org/10.1515/amsc-2017-0034

[5] Y. Cheng, H. Jiang, X. Zhang, J. Cui, C. Song, X. Li, *Effects of Coal Rank on Physicochemical Properties of Coal and on Methane Adsorption*. Int. J. Coal Sci. Technol. **4** (2), 129-146 (2017). DOI: https://doi.org/10.1007/s40789-017-0161-6

[6] Y. Tan, Y. Yin, G. Teng, *Simulation Research of Gas Seepage Based on Lattice Boltzmann Method*. J. China Coal Soc. **39** (8), 1446-1454 (2014). DOI: https://doi.org/10.13225/j.cnki.jccs.2014.9020

[7] V. Mishra, N. Singh, *Microstructural Relation of Macerals with Mineral Matter in Coals From is Valley and Umaria, Son-Mahanadi Basin, India*. Int. J. Coal Sci. Technol. **4** (2), 191-197 (2017). DOI: https://doi.org/10.1007/s40789-017-0169-y

[8] C. Zhang, X. Liu, X. Wang, *Combination Response Characteristics of Gas Seepage Velocity-Temperature Under Triaxial Loading*. J. China Coal Soc. **43** (3), 743-750 (2018). DOI: https://doi.org/10.13225/j.cnki.jccs.2017.0735

[9] J. Wei, L. Wei, D. Wang, *Experimental Study of Moisture Content Influences on Permeability of Coal Containing Gas*. J. China Coal Soc. **39** (1), 97-103 (2014). DOI: https://doi.org/10.13225/j.cnki.jccs.2013.0209

[10] D. Zhang, *Effect Analysis of Temperature on Seepage Characteristics Between Moulded Coal and Raw Coal*. Safe Coal Min. **49** (4), 152-155+159 (2018). DOI: https://doi.org/10. 13347/ j.cnki.mkaq.2018.04.040

[11] Y. Cai, X. Yang, Z. Tao, Q. Li, *Experimental Study on Creep Seepage Coupling of Coal and Rock Containing Gas*. Safety Coal Min. **47** (12), 19-22 (2016). DOI: https://doi.org/10.13347/j.cnki.mkaq.2016.12.006

[12] D. Wang, M. Peng, J. Wei, *Development and Application of Tri-Axial Creep-Seepage-Adsorption and Desorption Experimental Device for Coal*. J. China Coal Soc. **41** (3), 644-652 (2016). DOI: https://doi.org/10.13225/j.cnki.jccs.2015.0659

[13] J. Wei, S. Wu, D. Wang, F. Li, *Seepage Rules of Loaded Coal Containing Gas Under the Coupling Effect of Temperature and Axial Deformation*. J. Min. Safety Eng. **32** (1), 168-174 (02015). DOI: https://doi.org/10.13545/j.cnki.jmse.2015.01.027

[14] Z. Zhang, B. Cheng, *Study of a Non-Linear Seepage Model of Coal Containing Gas*. J. China U. Min. Techno. **44** (3), 453-459 (2015). DOI: https://doi.org/10.13247/j.cnki.jcumt.000327

[15] X. Yang, Z. Tao, B. Cai, Y. Lu, *Numerical Simulation on Fluid-Solid Coupling of Gassy Coal and Rock*. J. Liaoning Technical Univ. (Nat. Sci). **33** (8), 1009-1014 (2014). 2014. DOI: https://doi.org/10.3969/j.ssn.1008-0562.2014.08.001

[16] L. Min, Z. Bin, *Cartesian Closed Categories of FŹ-Domains*. Acta. Math. Sin. **29** (12), 2373-2390 (2013). DOI: https://doi.org/CNKI:SUN:ACMS.0.2013-12-014

[17] B. Zhao, G. Wen, H. Sun, D. Sun, H. Yang, J. Cao, L. Dai, B. Wang, *Similarity Criteria and Coal-Like Material in Coal and Gas Outburst Physical Simulation*. Int. J. Coal Sci. Technol. **5** (2), 167-178 (2018). DOI: https://doi.org/10.1007/s40789-018-0203-8

[18] V.T. Presler, *Modeling of Air-Gas and Dynamic Processes in Driving Development Workings in the Gas-Bearing Coal Seams*. J. Min. Sci. **38** (2), 168-176 (2002). DOI: https://doi.org/10.1023/A:1021167606258

[19] L. Sahu, S. Dey, *Enrichment of Carbon Recovery of High Ash Coal Fines Using Air Fluidized Vibratory Deck Separator*. Int. J. Coal Sci. Technol. **4** (3), 262-273 (2017). DOI: https://doi.org/10.1007/s40789-017-0172-3

[20] S. Nazary, H. Mirzabozorg, A. Noorzad, *Modeling Time-Dependent Behavior of Gas Caverns in Rock Salt Considering Creep, Dilatancy and Failure*. Tunn. and Undergr. Sp. Tech. **33** (1), 171-185 (2013). DOI: https://doi.org/10.1016/j.tust.2012.10.001

[21] L. Sahu, S. Dey, *Enrichment of Carbon Recovery of High Ash Coal Fines Using Air Fluidized Vibratory Deck Separator*. Int. J. Coal Sci. Technol. **4** (3), 262-273 (2017). DOI: https://doi.org/10.1007/s40789-017-0172-3

[22] W. Tanikawa, T. Shimamoto, *Comparison of Klinkenberg-Corrected Gas Permeability and Water Permeability in Sedimentary Rocks*. Int. J. Rock Mech. Min. **46** (2), 229-238 (2009). DOI: https://doi.org/10.1016/j.ijrmms.2008.03.004

[23] B. Zhang, X. Xie, Y. Liu, *Numerical Simulation on Gas Seepage in Front of Working Face Based on Fluid-Solid-Heat Coupling*. J. Safety Sci. Tech. **14** (3), 89-94 (2018). DOI: https://doi.org/10. 11731/ j.issn.1673-193x.2018.03. 013

[24] M. Mlynarczuk, M. Wierzbicki, *Stereological and Profilometry Methods in Detection of Structural Deformations in Coal Samples Collected from the Rock and Outburst Zone in The "Zofiowka" Colliery*. Arch. Min. Sci. **54** (2), 189-201 (2009). DOI: https://doi.org/10.2110/jsr.2014.48